Surface & Coatings Technology xxx (2012) xxx–xxx

Contents lists available at SciVerse ScienceDirect

Surface & Coatings Technology

journal homepage: www.elsevier.com/locate/surfcoat

Characterization of a MEMS tribogauge

Ashwin Vijayasai, Ganapathy Sivakumar, Gautham Ramachandran, Charlie Anderson, Richard Gale, Tim Dallas *

Electrical and Computer Engineering, Texas Tech University, Lubbock, TX, USA

ARTICLE INFO

Available online xxxx

Keywords:
Tribology
Adhesion force
Stiction
Friction
Coatings
MEMS

ABSTRACT

A MEMS tribogauge was used for on-chip and in-situ characterization of nano-tribological phenomena (stiction, friction, and wear). The measurements were made on the sidewall surfaces on the tribogauge at the third structural polysilicon layer in the device. The device consists of two orthogonally oriented comb-drive mechanisms that are used for both actuation and sensing functions. One actuator applies a normal load (F_n) to a contacting surface, while the other actuator induces a tangential load (F_T). A LabVIEW controlled AD7747 capacitance sensor is used to measure the position of the interacting surfaces. This data is converted into adhesive force information. The spatial resolution of the characterization apparatus is ±10 nm. Experiments were conducted with tribogauges with and without a self-assembled monolayer (SAM) coating. The SAM coatings being explored have a fluorocarbon tail group. The tribogauge with no SAM coating is UV/Ozone cleaned to remove organic contaminants. The tribogauge characterization includes: measurement of baseline stiction force $F^{FOTS}_{baseline}$, static (F_S) and dynamic (F_D) coefficient of friction, and induced stiction force $F^{FOTS}_{induced}$. The UV/Ozone treated tribogauge was used to measure the baseline stiction force. Additional experiments showed that the induced stiction force increases in proportion to the increase in the number of load cycles, indicating degradation of the SAM coating and inducing surface topographical changes to the interacting surfaces.

1. Introduction

Microelectromechanical systems (MEMS) have moving parts that can travel from sub-micrometer to a few micrometers for each input pulse. For example, an electrothermal actuator (chevron) can travel up to 10 μm [1]. Rotational gears designed in the SUMMiT-V [2] process can operate for millions of rotary cycles [3]. In each rotational cycle, contacting surfaces slide against each other in the hub region. If either the acting force or restoring spring force in the MEMS device (contacting and sliding devices only) is less than the surface adhesive force, the device fails to operate. Since the surface adhesive forces can be a showstopper for MEMS devices, a tribology study becomes important for MEMS [4]. Nano-tribology is the study which involves measurement of nano-tribological phenomena such as adhesion, friction and wear of surfaces under relative motion.

Surface adhesive force can be minimized by either physical modification or chemical modification of the surface. Physical modification of the surface is usually achieved in the fabrication process. By creating rough surfaces, contacting area can be reduced resulting in lower adhesive force. Chemical modification is preformed as a post fabrication step. In chemical modification, a chemisorbed layer on MEMS surface can alter adhesive properties of contacting surfaces [5]. Chemical modification of MEMS surface has proved to be a commercial success for reliable operation of Texas Instruments — Digital Micromirror Device (DMD). Since the DMD mirrors have several thousand contacting cycles every second, a low-surface energy coating becomes necessary for the operation of these devices. Several chemistries were evaluated by Texas Instruments for their DMD product [6]. One of the most popular chemical modification methods is deposition of a self-assembled monolayer on MEMS devices. Researchers have studied several monolayer nanocoatings for MEMS devices. Studies were either performed on nanocoated MEMS devices [7] or nanocoated sample surfaces (such as silicon wafer pieces). All the nanocoated sample surfaces are characterized using commercially available tools such as a nano-indenter, an atomic force microscope [8], an interferometric microscope, an electron microscopy, and a contact angle goniometer.

The atomic force microscope (AFM) is a powerful tool to measure surface forces [9]. Using pull-off force measurements, the adhesion force of MEMS surfaces can be measured. Nano-tribology studies can be performed on MEMS surfaces using AFM. However, the main drawback of this device is the study is performed on the interaction between the AFM probe material and the MEMS surface material. By using dissimilar materials to study tribology, uncertainty is introduced in the measured adhesion and friction values. To overcome this issue, several researchers have designed MEMS tribometers, which measure stiction and friction forces between the actual contacting surfaces.

* Corresponding author. Tel.: +1 806 742 3533x255; fax: +1 806 742 1245.
E-mail address: tim.dallas@ttu.edu (T. Dallas).

0257-8972/$ – see front matter © 2012 Elsevier B.V. All rights reserved.
http://dx.doi.org/10.1016/j.surfcoat.2012.07.089

Some of the early MEMS tribometer designs include capacitance based cantilevers; the most recent ones are designed using comb-fingers. Mastrangelo et al. [10] were the first to measure stiction forces between structural layers using bent cantilever beams. de Boer et al. used a specially designed "hinge-pad test structure" to determine sliding friction [11]. A wobble motor was used to obtain the magnitude of the friction force by monitoring the actuation voltage required for inducing the motion of the motor by Lim et al. [12] and Mehregany et al. [13]. Prasad et al. [14] and Sneft and Dugger [15] were among the first to measure the dynamic friction on sidewall surfaces. Sneft and Dugger used optical techniques to obtain the dynamic friction coefficient from their devices. de Boer et al.'s version of a MEMS tribometer, the "Nanotractor," was used to obtain the static friction coefficient for varying normal loads. It was used for comprehensive tests with different coating materials [16].

The objective of this work is the development of a MEMS chip-based characterization tool to be used for in-situ studies and quantification of nano-tribological parameters including stiction, friction, and wear. In this paper, the design of the 'MEMS Tribogauge' and details of the characterization setup are presented. Other researchers have made significant progress in the study of adhesion; friction and wear for sidewall MEMS surfaces [14,17–21]. Major characteristic features of our device are: our tribogauge design occupies a relatively small area on the MEMS chip ~550×600 μm (out of ~2800×6200 μm), the smallest tribometer found in the literature is at least 100% larger than our device [18]. There is no linkage between the normal axis comb drive and lateral axis comb-drive. This leads to individual measurement of the normal and lateral forces. Design by Sneft and Dugger [15] had the lateral and normal axis tied together. They had to implement post-process calculations to precisely measure the adhesion forces. By using Sandia's high performance comb-drive, more force can be generated and there can be more sense capacitance per unit area. Our comb-drive does not undergo the levitation effects as described by Spengen et al. [19]. We have verified this experimentally using an interferometry tool. Other tribometer designs [12,15,16,18,19] have a 'double-fold spring system,' which has a dimple contacting the bottom poly-Si surface. When these devices are under operation, the surface–surface interaction between a dimple and the bottom poly-Si will add to the measured stiction force. This corresponds to adding noise to the absolute stiction force. In our design, the high performance comb-drive does not have this issue. Hence our design will measure authentic stiction force between the actual reference surfaces.

2. MEMS tribogauge description

2.1. Design

The 'MEMS tribogauge' is fabricated using Sandia National Laboratories SUMMiT-V process [2]. A scanning electron image of the fabricated device is shown in Fig. 1. In the SUMMiT-V process, five polysilicon layers are used; four layers are used as structural layers (labeled 'MMPOLY1 to 4') and one layer is used for anchoring purposes/electrical connections (labeled 'MMPOLY0'). The comb-drive assemblies used in this design are referred to as high performance comb-drive actuators (HPCD), which are included as "library parts" in Sandia's design tool plug-ins for the AutoCAD software.

These actuators utilize all the mechanical layers of polysilicon for the comb-drive fingers, the central shuttle, and the supporting spring assemblies. The detailed explanation of the suspension system is provided by Rogers et al. [22]. The stationary combs are anchored to the substrate while the movable combs are suspended by the springs. The comb fingers are arranged as comb banks. A total of 16 comb-banks are included in the design. Each comb bank has 20 pairs of comb fingers. 8 comb-banks are stacked in the Y axis while the remaining 8 comb-banks are stacked in the X axis. The 8 comb-banks in the X and Y axes are equally divided as actuation and sense assemblies. Both X and Y axis comb-drive assemblies are arranged orthogonally and the interacting surfaces between them (in MMPOLY3) gauge the tribological phenomena. The X-axis comb-assembly is divided into two parts and joined through a beam connected to the push head of one assembly at one end and pull head of the second assembly on the other end. The normal load between the references surfaces used for measurements is applied by the Y-axis assembly while the lateral force to initiate lateral load between the surfaces is applied by the X-axis assembly.

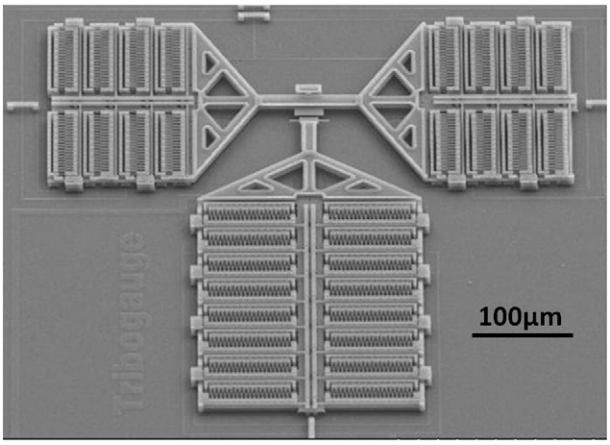

Fig. 1. SEM image of 'MEMS tribogauge'.

The comb fingers used in both the X and Y axes have the same number of actuation fingers and sense fingers. The electrostatic force generated by the comb-drives for both X (F_x^e) and Y (F_y^e) axes are given by [22]:

$$F_y^e = F_x^e = F_{tot.} = \frac{N\varepsilon t}{g} V^2 \quad (1)$$

where, N = number of actuation fingers in the comb-drive = 80, V is the driving voltage, $\varepsilon = \varepsilon_o \cdot \varepsilon_r$ = product of permittivity of free space (8.854×10^{-12} F/m) and relative permittivity (1), respectively, t = thickness of each finger ~7×10^{-6} m, and g = gap in-between movable and anchored fingers which is ~0.9×10^{-6} m.

The support springs in the comb-drives produce a restoring force which is equal in magnitude to the applied electrostatic force. The restoring force in both X (F_x^e) and Y (F_y^e) axes is given by Hooke's law:

$$F_y^e = F_y^e = K^*\delta \quad (2)$$

where, $k = K_x = K_y$ = spring constant and δ = linear displacement made by actuator (δ_x for the X axis actuator and δ_y for the Y axis actuator).

2.2. Operation

The tribogauge device can be used for in-situ stiction, friction and wear studies. Measurement of stiction and friction forces between reference surfaces is illustrated in Fig. 2. In Fig. 2, 'surface 1' is the surface on the protrusion of MMPOLY3 in the Y axis, and 'surface 2' is on the X beam of MMPOLY3 in the X axis. The Y protrusion (labeled 'Y HEAD') can be actuated to apply a normal load between the surfaces, while the X beam (labeled as 'X HEAD') can be actuated to induce lateral motion between the surfaces.

In the first mode represented in Fig. 2(a), wherein the device is used to quantify stiction force at the contact, the actuator associated with surface 1 (Y HEAD.) is initially in the power-off state and the two surfaces are not in contact with each other (Fig. 2(a) '1'). In the

Please cite this article as: A. Vijayasai, et al., Characterization of a MEMS tribogauge, Surf. Coat. Technol. (2012), http://dx.doi.org/10.1016/j.surfcoat.2012.07.089

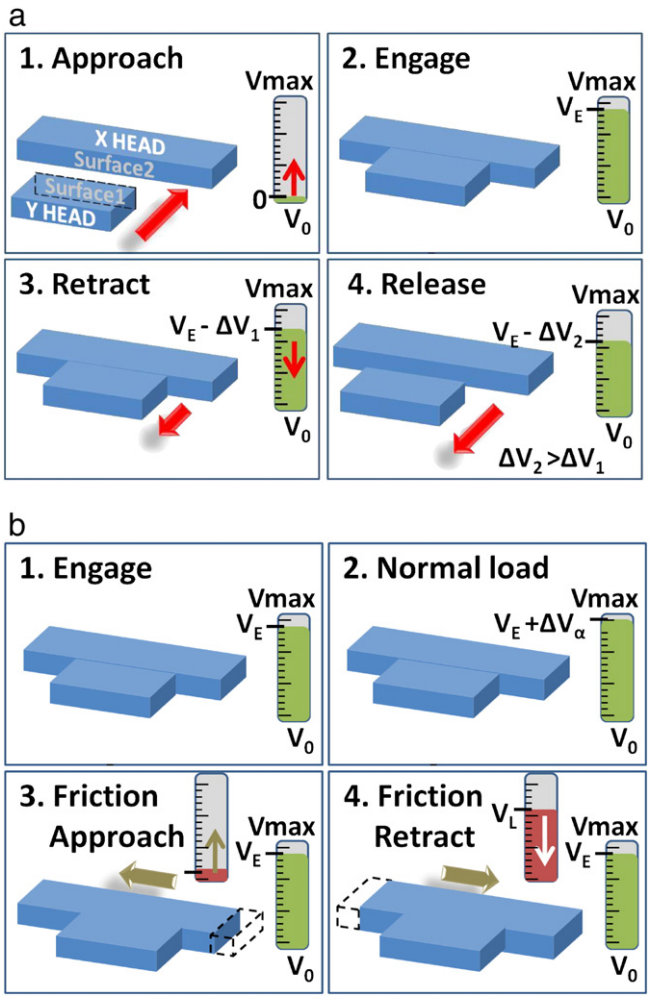

Fig. 2. Illustration of (a) stiction measurement and (b) friction measurement.

approach cycle, the actuator connected with the slider is powered on with an increasing DC voltage. The point at which both the surfaces are in contact is recorded as the engage point. This happens at a DC signal of V_E volts (Fig. 2(a) '2'). If the DC signal is increased beyond V_E, a normal load force is applied on surface 2. The value of the 'normal load force' is proportional to the DC signal greater than V_E. In the retract cycle, the DC signal is decreased below the engage point V_E. In both approach and retract cycles, the step change of the applied DC signal is ΔV_α. It is observed that the point of release occurs at a step value of ΔV_2 which is greater than ΔV_1 (Fig. 2(a) '3' and '4'). The difference in the point where the contact was established and the point where the contact was lost will provide information regarding the stiction force acting between the contacting surfaces.

In the second mode of operation, as represented in Fig. 2(b), the friction between the surfaces in contact can be studied. In order to quantify friction, the first step is to achieve the engage point (Fig. 2(b) '1'); this is similar to the explanation of the first mode (Fig. 2(a) '2'). The normal force acting at the contact can be controlled by the applied DC signal on the comb-drive actuators connected to surface 1. The applied normal force is proportional to ΔV_α (Fig. 2(b) '2'). Once the surfaces are brought into contact with each other with a pre-determined contacting force, the actuators on surface 2 are powered up with a DC voltage to induce a lateral motion between the contacting surfaces (Fig. 2(b) '3' and '4'). The difference between the displacement versus voltage curve when surfaces are in contact versus when not in contact provides information regarding the friction force between the surfaces. The frictional force depends on both the sliding distance of X HEAD and the normal force applied by the Y HEAD.

3. Experimental test setup

3.1. Experimental setup

The experimental setup used in the measurement of capacitance from the tribogauge is shown in Fig. 3. The tribogauge device along with an array of ~20 other devices is fabricated on a single MEMS chip. This chip is wire-bonded on a 48pin DIP sealed with a glass lid. A capacitance sense board from Analog Device's model#AD7747-EB is used to sense capacitance values from the tribogauge. A Honeywell–HIH 4000-001 sensor is used to measure relative humidity (R.H.). Capacitance read-out and relative humidity values are recorded in log files. Measurement of the change in capacitance with respect to step increments of actuation voltage will produce results in the femtofarad range. Characterization of the capacitance sensor board showed an error ~±110 aF. This value corresponds to a displacement value of ~±10 nm.

3.2. Evaluation of the setup measurements with accurate dimensions

The origin of electrostatic forces and the counteracting spring restoring forces in the tribogauge depends on critical dimensions of the fabricated device. It is important to minimize approximations while measuring nano-scale tribological phenomena. Our current electrical characterization setup demands accurate inputs of tribogauge dimensions, while using it as the 'device under test.' We have measured the critical dimensions using an electron microscope from Hitachi (#S3400N). These dimensions were incorporated in the calculations and results are compared for FEA analysis against measured capacitance values.

The capacitance of the comb-drive mechanism can be calculated from the equation:

$$C = \frac{\varepsilon . A}{g} = N \cdot \frac{\varepsilon_o \varepsilon_r (tl)}{g} \tag{3}$$

where, N = total number of comb-fingers = 80; ε_o = permittivity of free space = 8.854×10^{-12} F/m; ε_r = relative permittivity = 1; t = thickness of each finger ~7×10^{-6} m; g = gap in-between movable and anchored fingers ~0.7×10^{-6} m; l = overlap length of comb fingers (displacement in μm).

We have performed electrostatic modeling on one pair of comb-finger with COMSOL multi-physics software. The drive capacitance of the entire comb-drive assembly is approximated by multiplying the

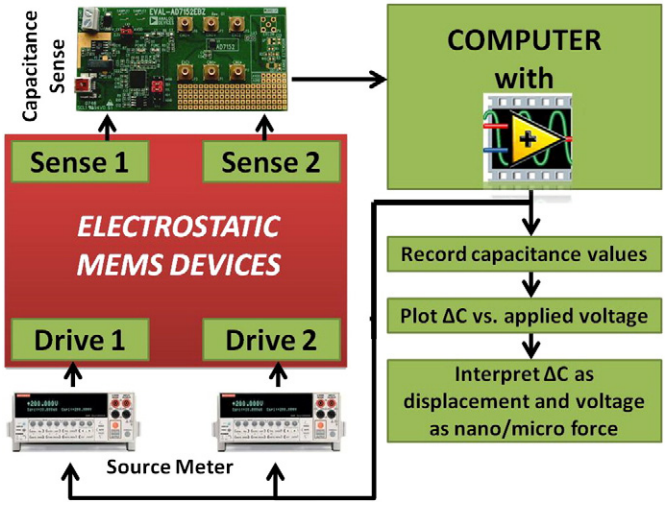

Fig. 3. Outline of the electronic characterization setup. This setup can be used for tribogauge which has two drives and two sense connections in X and Y axis .

Please cite this article as: A. Vijayasai, et al., Characterization of a MEMS tribogauge, Surf. Coat. Technol. (2012), http://dx.doi.org/10.1016/j.surfcoat.2012.07.089

result with the total number of comb-fingers. The fringing field effect is neglected in the model. The geometry of both the AutoCAD design and the measured design are modeled in the software. Fig. 4 shows capacitance of simulated values and experimentally measured values as a function of displacement. The simulation results of the AutoCAD design dimensions (ii) show a maximum variation of ~57fF with fabricated design dimensions (iii). This implies that post-fabrication inspection of dimensions is important for quantifying micro/nano adhesion forces. Experimentally measured values (i) fall in-between (ii) and (iii), but are closest to (iii). For experimentally measured values, both electronic sensing and optical characterization schemes were used. A total of four chips were used in the experimental measurements.

Comparing Eqs. (1) and (3) a relationship between applied force and capacitance is found:

$$F_{tot.} = \left(\frac{C.V^2}{l}\right). \quad (4)$$

Evaluating the performance of our electronic sensing setup, we have calculated the variation in applied force to be 10.4nN, i.e., ± 1.8% of the measured value.

3.3. Spring constant calculation and levitation effects

The value of the spring constant, K, is calculated to be 20.0 μN/μm for both axes ($K_x = K_y$). An optical system (Olympus #BX60 microscope) was used for capturing images and post process image software (National Instruments - Automated Inspection) was used to calculate the spring constant.

In a comb-drive actuator, a levitation force can induce variation in expected device motion. In stiction experiments, the variation of device motion can lead to inaccurate results [23]. A Veeco # NT1100 interferometric microscope was used to determine surface topography. The results suggest the absence of levitation effects in our device.

4. Results and discussion

4.1. Experiment 1 — baseline stiction force

For baseline stiction force measurement, a pristine tribogauge device is used. The measured stiction force is the aggregate of the various interfacial forces. The interfacial forces scale with the topography of the contacting surfaces. For stiction measurements, the normal axis of the tribogauge is actuated using a DC signal. The basic operation was described earlier; DC signal (0–45 V) is applied to the device in increments of $\Delta V_\alpha = 100$ mV. At every increment, the capacitance is measured from the sense comb-fingers. A LabVIEW GUI is used to control the actuation and sensing functions.

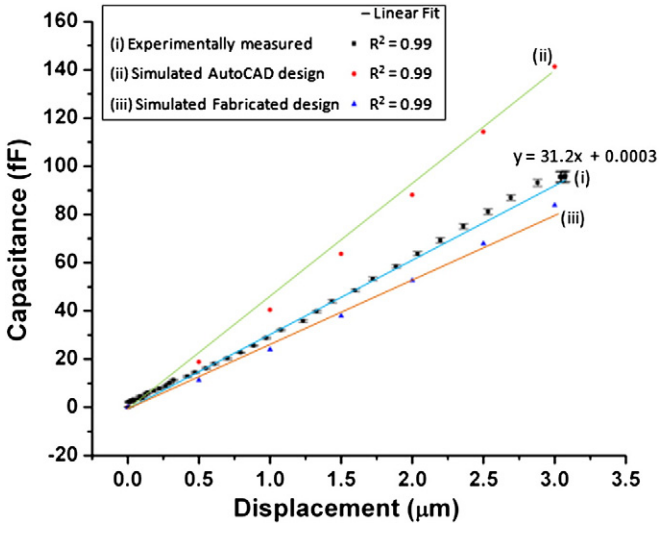

Fig. 4. Comparison of capacitance vs. displacement values for simulation; experimentally measured values.

During the approach cycle (0–45 V), the point when the capacitance reaches saturation is called the pull-in point. During the retract cycle (45–0 V), the point at which the capacitance readout begins to measure values greater than pull-in is called the pull-off point. By observing the approach and retract curves, there is a region of discontinuity. This region gives information on stiction force calculation. In this region, there is a point where the capacitance change is greater than ±110 aF per decremented step. This point is called the release point.

By observing the capacitance values from the capacitance readout mechanism, the pull-in, pull-off, and release points can be identified. The quantified measurement of force at the release point equals to the stiction force.

The stiction force can be obtained from Eq. (4):

$$F_{stiction} = F_{pull\_}in - F_{pull\_}off = \left[\frac{\left(C_{pull\_}in - C_{pull\_}off\right)\cdot\left(V^2_{F_{pull\_}in} - V^2_{F_{pull\_}off}\right)}{\left(l_{pull\_}in - l_{pull\_}off\right)}\right] \quad (5)$$

where, $F_{pull\text{-}in}$ = Force experienced by the comb-drive mechanism during the approach cycle; $F_{pull\text{-}off}$ = force experienced by the comb-drive mechanism during the retract cycle; $V_{pull\text{-}in}$ = approach voltage at the pull-in point; $C_{pull\text{-}in}$ = approach capacitance at the pull-in point; $l_{pull\text{-}in}$ = approach displacement of the comb fingers at the pull-in point; $V_{pull\text{-}off}$ = retract voltage at the pull-off point; $C_{pull\text{-}off}$ = retract capacitance at the pull-off point; $l_{pull\text{-}off}$ = retract displacement of comb-fingers at the pull-off point. The values of $l_{pull\text{-}in}$, $l_{pull\text{-}off}$ are not measured optically, instead they are calculated from the trend-line equation of (i) in Fig. 4.

The devices received from Sandia National Labs are 'dry cleaned' using a UV-O tool (Model # Novascan PSPD UV-4), for a duration of 20 min. Then, the devices are placed inside a nanocoating tool (Integrated Surface Technologies #RPX-550). The devices are coated with per-fluoro-octly-trichlorosilane (FOTS). The stiction force was found to be $F^{FOTS}_{baseline} \sim 120 \pm 10$ nN. All the cleaning and measurements were performed in a lab environment at 25 °C and 35% R.H. The contacting area used during the experiment was 44.4 μm^2. For any pristine device, the first measurement of stiction force is termed baseline stiction (Fig. 5).

4.2. Experiment 2 — induced stiction by scrub loading with constant normal load

First, the baseline stiction force is measured for the tribogauge. Then, the stiction force is measured as a function of increasing scrub load cycles. In a scrub load, the normal load force of ~1.9 μN is applied followed by a tangential load force ~27.7 μN at various frequencies. The various frequencies followed in the experiment are 1 Hz (from 1 to 10 load cycles), 5 Hz (from 20 to 100 load cycles) and 100 Hz (beyond 100 load cycles). The load cycles are in logarithmic progression, stiction force is measured after every load cycle. The values of measured stiction force against load cycle are shown in Fig. 6. Experiments were carried out for a pristine tribogauge device (coated with FOTS SAM) at 25 °C and 35% R.H. Overall, it was observed that the stiction force increased as a function of load cycles.

The values reported in Fig. 6 are measured for one device. The Y error bars has a maximum value of 15 nN. The measured values have very few quantized locations compared to normal load experiment. To confirm this response, two more devices were tested (results not shown in Fig. 6). A similar increase in stiction force was

Please cite this article as: A. Vijayasai, et al., Characterization of a MEMS tribogauge, Surf. Coat. Technol. (2012), http://dx.doi.org/10.1016/j.surfcoat.2012.07.089

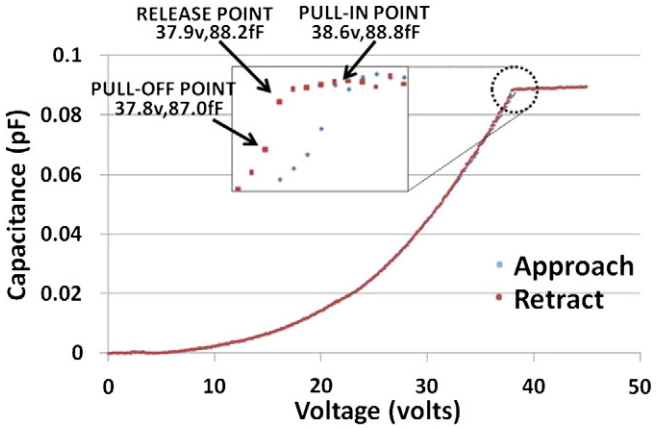

Fig. 5. Sample plot showing magnified portion of the plot indicates the pull-in, release and pull-off points.

observed. From 1 to 1E7 load cycles, the measured stiction forces between three devices varied between ±45 nN and ±650 nN. Assuming conformal coverage of the SAM in tribogauge devices, we suspect the variance is mainly caused by different topologies of the interacting surfaces.

Observations from Fig. 6:

Table 1 summarizes the value of data points at every load cycle in Fig. 6. Some of the major observations are:

(i) There is a small increase in the stiction force in the first 5 load cycles (131 nN). The increasing response is polynomial.
(ii) From load cycle 6 to 70 the stiction force is constant, but it again gradually increases from 80 to 100 load cycles (131 nN). The increasing response is polynomial.
(iii) From load cycle 200 to 1.0E6 the stiction force increases steadily (910 nN). The increase response is linear.
(iv) Again from 2.0E6 to 1.0E7 the behavior of stiction force is polynomial. The increase is steep in this region (~1020 nN).

Optical observations of FOTS coated device after 1.0E7 load cycles reveal no particle debris on the "Y HEAD" and "X HEAD."

4.3. Experiment 3 — friction measurement

4.3.1. Dynamic friction test

First, the X axis comb drive is powered with a sine–wave voltage signal while the Y axis comb drive actuator is unpowered. In this motion, both the 'X and Y HEADS' are out of contact. The maximum displacement of the X axis comb drive is represented as d_O. Next, the Y axis comb drive actuator is powered with a specific normal load (a few nN) followed by lateral comb drive oscillations at the same oscillating voltage signal. In this motion, both 'surface1' and 'surface2' are in-contact. The maximum displacement of the X axis comb drive is represented as d_I.

From experiments, the friction force can be measured as:

$$F_d = \frac{1}{2}\cdot k_x(d_O - d_I) \tag{6}$$

where, k_x = spring constant of X axis comb drive. During the experiment, the friction force is generated during the approach and the retract cycle (Fig. 2(b) '3' and '4'). Hence, the friction force (F_d) in Eq. (6) is divided by two.

By Derjaguin's modified version of Amonton's equation, the friction force between adhering surfaces is given by [16]

$$F_d = \mu_d\left(F_{stiction} + F_y^L\right) \tag{7}$$

where, $F_{stiction}$ = stiction force between the interacting surfaces (in Newtons), F_y^L = Y axis load force (in Newtons) and μ_d = coefficient of dynamic friction.

From Eqs. (6) and (7):

$$\mu_d = \frac{1}{2}\cdot\frac{k_x(d_O - d_I)}{F_{stiction} + F_y^L}. \tag{8}$$

For a pristine tribogauge with FOTS SAM coating, calculations for Eqs. (7) and (8) shows that $F_d = 19.4$nN and $\mu_d = 0.02 \pm 0.01$ (when F_y^L~670 nN, $F_{Stiction}$~300 nN) respectively. The same device after

Table 1
Summary of Fig. 6.

S.No	Load cycle	FOTS coating		
		Stiction force (nN)	Increase in stiction force	
			Range	Δ stiction force (nN)
A	1.0E0	132	–	–
B	1.0E1	263	A to B	131
C	1.0E2	395	B to C	132
D	1.0E3	656	C to D	261
E	1.0E4	786	D to E	130
F	1.0E5	1045	E to F	260
G	1.0E6	1304	F to G	260
H	1.0E7	2323	G to H	1019

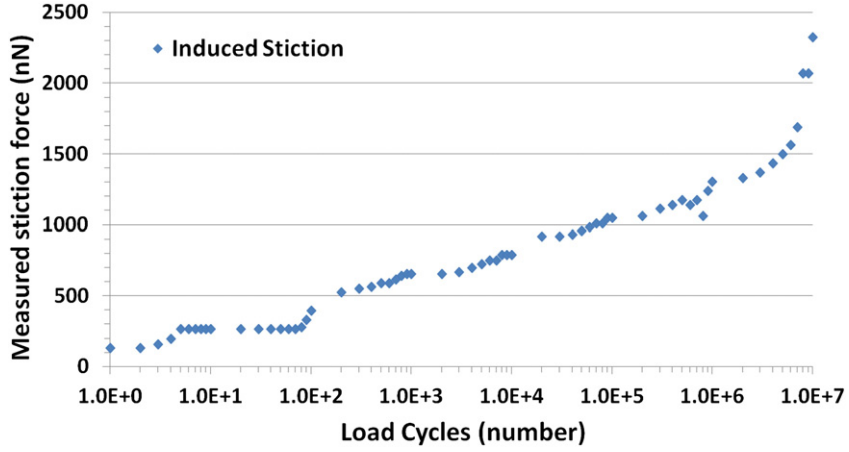

Fig. 6. Plot of measured stiction force against scrub load cycle. The scale for FOTS and SVSAM data points are in right and left sides respectively. $F_{baseline}^{FOTS}$ ~132 nN and $F_{baseline}^{UV\text{-}O}$ ~4.43 ± 0.02 μN.

Please cite this article as: A. Vijayasai, et al., Characterization of a MEMS tribogauge, Surf. Coat. Technol. (2012), http://dx.doi.org/10.1016/j.surfcoat.2012.07.089

10,000 scrub cycles (tangential sliding force ~27.7 μN, F_y^L ~1.90 μN and $F_{Stiction}$ ~800 nN) showed $F_d = 486$ nN and $\mu_d = 0.18 \pm 0.02$.

4.3.2. Static friction test

When the X HEAD and Y HEAD surfaces are under fixed normal and tangential loads, respectively, the force required to initiate sliding between the surfaces is called static friction. Unlike the dynamic friction test, in this test a specific load is applied on the Y axis comb drive actuator, F_y^L and the X axis is powered at small steps of 100 mV (corresponding to F_x^L). The static friction coefficient is defined as the ratio of X axis force which initiates sliding between scrubber and slider surfaces ($F_{x\ init.}$) and Y axis load ($F_{stiction.} + F_y^L$).

$$\mu_s = \frac{F_x \text{init.}}{\text{Fstiction} + F_y^L} \tag{9}$$

Where, μ_S = coefficient of static friction.

Also the instant when the tangential force $F_{x\ init}$ overcomes the collective force of adhesion and Y axis load is measured as static friction force F_S.

$$F_s = \mu_s \left(F_{stiction} + F_y^L\right) \tag{10}$$

For a pristine tribogauge with FOTS SAM coating, calculations for Eqs. (9) and (10) shows that $\mu_S = 0.04 \pm 0.01$ and $F_S = 52.8$ nN respectively (when F_y^L ~1.02 μN, $F_{Stiction}$ ~300 nN). The same device after 10,000 scrub cycles (F_x^L ~27.7 μN, F_y^L ~1.90 μN and $F_{Stiction}$ ~800 nN) showed $\mu_S = 0.20 \pm 0.01$ and $F_S = 540$ nN respectively.

5. Conclusion

This work demonstrates characterization of a MEMS tribogauge coated with FOTS coating. We have performed several experiments using this device. The tribogauge devices coated with FOTS and no SAM coating were all tested for the Baseline stiction force. $F_{baseline}^{FOTS}$ ~120 ± 10 nN, for a UV-O cleaned device the stiction force is 37.5 times higher. For tribogauge devices coated with FOTS coatings, induced stiction force is measured as a function of scrub load. After 10,000 scrub load cycles the stiction force increased five times. Static and dynamic coefficients of friction are determined for a FOTS coated tribogauge. The static coefficient of friction for a pristine device is F_s^{FOTS} ~0.04 ± 0.01, but after 10,000 scrub cycles the value was five times higher. The dynamic coefficient of friction for a pristine device is F_d^{FOTS} ~0.02 ± 0.01. After 10,000 scrub cycles a 9-fold increase in force was measured.

Acknowledgment

The authors acknowledge support from a National Science Foundation MRI grant (CBET #0821162) and Sandia National Labs for fabricating the MEMS chips used in this work. The authors would like to thank Manjula Wickramasinghe and Dr. Jordan Berg, Department of Mechanical Engineering, Texas Tech University, for donating the AD7747-EB board; SEM/TEM images provided by Charles Linch, Texas Tech University Health Sciences Center Imaging Center.

References

[1] M.S. Baker, R.A. Plass, T.J. Headley, J.A. Walraven, in: Tech. Rep. LDRD #52553, SAND2004-6635, Sandia Nat. Lab., Albuquerque, NM, Dec. 2004.
[2] J.J. Sniegowski, M.S. Rodgers, in: 2nd International Conference on Engineering Design and Automation, Maui, Hawaii, 1998.
[3] J.J. Sniegowski, E.J. Garcia, IEEE Electron Dev. Lett. 17 (1996) 366.
[4] M.P. de Boer, T.M. Mayer, MRS Bull. 26 (2001) 302.
[5] J.G. Kushmerick, M.G. Hankins, M.P. de Boer, P.J. Clews, R.W. Carpick, B.C. Bunker, Tribol. Lett. 10 (2001) 103.
[6] S.A. Henck, Tribol. Lett. 3 (1997) 239.
[7] W.R. Ashurst, M.P. de Boer, C. Carraro, R. Maboudian, Appl. Surf. Sci. 735 (2003) 212.
[8] E. Hoque, J.A. DeRose, P. Hoffmann, B. Bhushan, H.J. Mathieu, J. Phys. Chem. C 111 (2007) 3956.
[9] E.J. Thoreson, J. Martin, N.A. Burnham, J. Microelectromech. Syst. 16 (2007) 694.
[10] C.H. Mastrangelo, C.H. Hsu, in: Inter. Work. on Solid-State Sens. and Act., Hilton Head, S.C., 1992.
[11] M.P. De Boer, J.M. Redmond, T.A. Michalske, Proc. SPIE 3512 (1998) 241.
[12] M.G. Lim, J.C. Chang, D.P. Schultz, R.T. Howe, R.M. White, Proc. IEEE Worksop Micro Electro Mech. Syst. 82 (1990) 11.
[13] M. Mehregany, S.D. Senturia, J.H. Lang, Proc. IEEE Solid-State Sens. Actuators Workshop 17 (1990) 10.
[14] R. Prasad, N. MacDonald, D. Taylor, in: Proc. Inter. Conf. on Solid-State Sens. and Act. TRANSDUCERS, 52, 1995.
[15] D.C. Sneft, M.T. Dugger, Proc. SPIE 3224 (1997) 3.
[16] A.D. Corwin, M.D. Street, R.W. Carpick, W.R. Ashurst, M.J. Starr, M.P. de Boer, in: Tech. Rep. SAND #2005-7954, SAND2004-6635, Sandia Nat. Lab., Albuquerque, CA, 2006.
[17] S.J. Timpe, K. Komvopoulos, J. Microelectromech. Syst. 14 (2005) 1356.
[18] S.J. Timpe, K. Komvopoulos, Rev. Sci. Instrum. 78 (2007) 065106.
[19] W.M. van Spengen, J.W.M. Frenken, Tribol. Lett. 28 (2007) 149.
[20] D.H. Alsem, M.T. Dugger, E.A. Stach, R.O. Ritchie, J. Microelectromech. Syst. 17 (2008) 1144.
[21] D.H. Alsem, R. van der Hulst, E.A. Stach, M.T. Dugger, J. De Hosson, M. Th, R.O. Ritchie, Sens. Actuators A Phys. 163 (2010) 373.
[22] S.M. Rodgers, S. Kota, J. Hetrick, Z. Li, B.D. Jensen, T.W. Krygowski, S.L. Miller, S.M. Barnes, S. Burg, Solid-State Sens. and Act. Hilton Head Island, , 2000.
[23] W.C. Tang, M.G. Lim, R.T. Howe, J. Microelectromech. Syst. 1 (1992) 170.

Please cite this article as: A. Vijayasai, et al., Characterization of a MEMS tribogauge, Surf. Coat. Technol. (2012), http://dx.doi.org/10.1016/j.surfcoat.2012.07.089